Nigerian Journal of Technology (NIJOTECH)
Vol. 41, No. 5, September, 2022, pp.854 - 861
www.nijotech.com

Print ISSN: 0331-8443
Electronic ISSN: 2467-8821
http://dx.doi.org/10.4314/njt.v41i5.5

EFFECT OF INDIUM VACANCY POINT DEFECT ON THE STRUCTURAL, ELECTRONIC AND OPTICAL PROPERTIES OF DOUBLE PEROVSKITE HALIDE $Cs_2InSbCl_6$

I. Magaji[1,*], A. Shuaibu[1], M. Isah[1], Y. A. Kauru[1], and A. Hussaini[1]

[1] Department of Physics, Faculty of Science, Kaduna State University, P.M.B, 2339, Kaduna, Nigeria.

*corresponding author (Email: imagaji05@gmail.com)

Article history: Received 29 March, 2022. Revised 19 May, 2022. Accepted 23 May, 2022

Abstract
Efforts to replace the lead-based perovskite have gain significant improvements in the last decade. Lead free double halide perovskite are being considered to replace the toxic lead-based perovskite materials for solar cell applications. Density functional theory (DFT) and linear response time-dependent density functional theory (TDDFT) are used in this study to simulate and investigate the effect of vacancy in the Indium (In) site of lead-free double halide perovskite $A_2BB'X_6$ (A = Cs; B = In, B′ = Sb; X = Cl) on the structural, electronic, and optical properties for possible solar cell application. On the structural properties, the total bond length of the material $Cs_2InSbCl_6$ was found to be 30.3848 Å and the creation of the indium vacancy raises the value to 30.594 Å. The bulk modulus of $Cs_2InSbCl_6$ was calculated to be 28.44 Gpa and 26.22 Gpa for $Cs_2In_{-x}SbCl_6$. The calculated band structure for $Cs_2InSbCl_6$ reveals semiconducting behavior with a direct energy band gap of 0.99 eV along Γ point symmetry while the created indium vacancy band structure reveals metallic behavior with an overlap of electronic states along the Γ - W – Γ symmetry. The result of the optical properties calculations shows that the material $Cs_2InSbCl_6$ has higher absorption coefficient, low refractive index, low reflectivity and higher conductivity when compared to the created indium vacancy material.

Keywords: Defect, Vacancy, Solar Cells.

1.0 INTRODUCTION

The lead-free halide double perovskite has the general formula of the form $A_2BB'X_6$ where B is a monovalent and B' is a trivalent cation, whereas A and X are monovalent cation and halide anion respectively. They have attracted significant attention and are considered excellent candidate to replace the toxic lead-based perovskite materials. Halide double perovskite such as $Cs_2InBiCl_6$ and $Cs_2InSbCl_6$ are predicted to be promising photovoltaic solar cell absorber material [1] due to their large absorption coefficient [2], low manufacturing cost [3], close-to optimal band gap, etc. [4]. They have numerous technological applications, such as light emitting diodes, solar cell absorbers, high efficiency thin film transistors, laser diodes, high density optical memories, etc. [5], this makes them attract vast interests owing to their current and potential future applications. These materials are recognized with great promise for photovoltaic because of their excellent quantum efficiency and high light sensitivity. First principle DFT calculation was used in this work to study the effect of Indium vacancy ($Cs_2In_{-x}SbCl_6$) point defect to control the REDOX reaction in $Cs_2InSbCl_6$ for potential solar cell application.

2.0 COMPUTATIONAL DETAILS

The first principle calculations were carried out within the frame work of DFT [6] and TDDFT [7] by the use of plane-wave (Pw) pseudopotential technique as implemented in quantum ESPRESSO suite [8]. Generalized gradient approximation (GGA) was used as exchange-correlation functional formulated by Perdew Burke Ernzerhof (PBE) [9]. The structural parameters (lattice parameters and internal atomic coordinate) were optimized and fully relaxed using

Broyden-Flectcher-Goldfarb-Shanno (BFGS) quasi-Newton algorithm [10]. 60 and 240 Ry were set for the convergence test of the kinetic energy cut-off for wave function and charge densities respectively. For defecting in the indium atomic site, an indium atom (x = 0.25) was forcefully removed from it atomic position and coordinate leaving a vacancy in the indium atomic site of the compound. The supercell dimensions are kept fixed throughout the calculations. The Monkhorst-pack k-point mesh sampling of Brillouin zone integration was set as 6 x 6 x 6 and a denser k-point mesh of 12 x 12 x 12 for density of state (DOS). 10^{-7} was set as the convergence threshold for self-consistent-field (SCF) iteration. Equation (1) was used to calculate the bulk modulus of the materials.

$$B_0 = -V_{dv}^{dp} = B_1 + B_2, B_1 = -V_{1(v_1-v_2)}^{(p_1-p_2)}, B_2 = -V_{1(v_1-v_3)}^{(p_1-p_3)} \quad (1)$$

Where B_0 is the bulk modulus, V is the volume of the structure, and p is the pressure (stress)

3.0 RESULT AND DISCUSSION

3.1 STRUCTURAL PROPERTIES

The $Cs_2InSbCl_6$ is a face-centered-cubic (FCC) lattice structure belonging to the space group Fm-3m. The simple primitive cell contains 10 atoms. However, a super cell of 40 atoms was used throughout the course of this work. The optimized crystal lattice parameters obtained are a = b = c = 11.342 Å and $\alpha = \beta = \gamma = 90^0$. The value obtained is in agreement with the experimental value 11.32 Å [1]. The defect raises the value of the crystal lattice parameters. Generally, energy gap is inversely proportional to the interatomic distance. The defect reduces the bond length between the Cs site (1) and the 3 In atoms sites from 2.4653 Å to 2.4586 Å, Cs site (1) and the 3 Cl atoms sites from 2.9474 Å to 2.8767 Å, Cs atom site (1) and Sb atoms sites from 4.3045 Å to 4.1015 Å. It thus increases the bond length between the Cs atom site (1) and 3 Cs atom sites from 2.8957 Å to 2.9222 Å. Decrease in bond length improves atomic bonding [11].

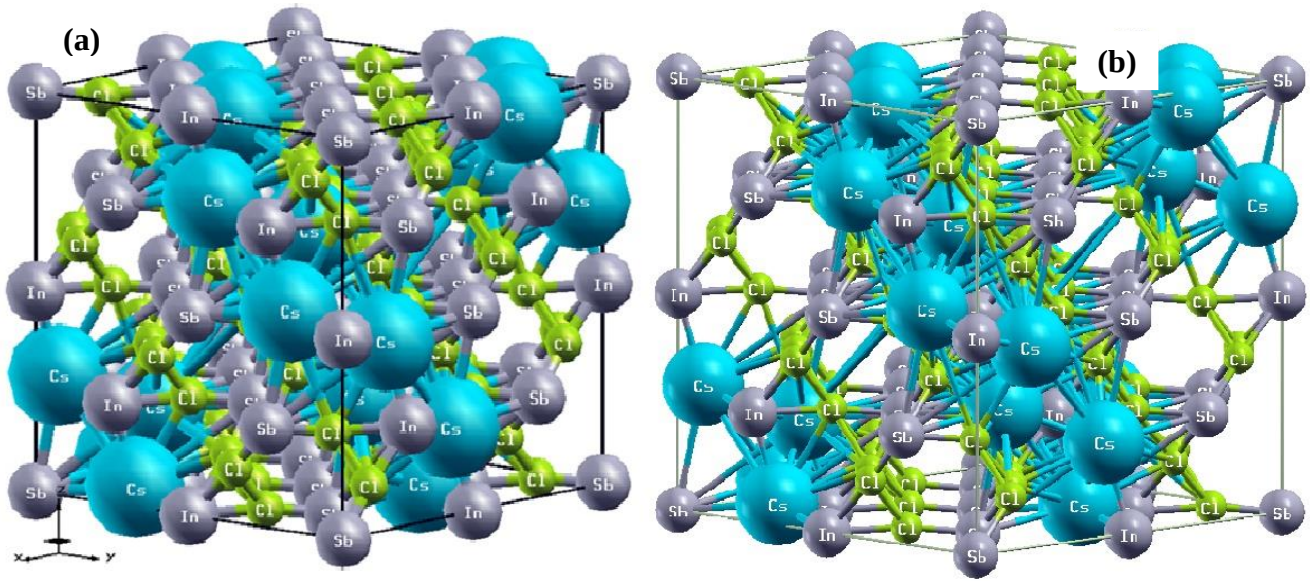

Figure 1: Crystal Structure of (a) $Cs_2InSbCl_6$ (b) $Cs_2In_{-x}SbCl_6$

The bulk modulus often defines material characteristics such as compressibility or flexibility, strength, hardness. The ability of a material to resist deformation under applied stress is often defined by its bulk modulus [12].The result of the calculated bulk modulus obtained using equation (1) reveals that the $Cs_2InSbCl_6$ has a bulk modulus value of 28.44 Gpa while $Cs_2In_{-x}SbCl_6$ has 26.22 Gpa, 2.22 Gpa lesser than the reference material. The result indicates that the material $Cs_2In_{-x}SbCl_6$ is more compressible and less hard [13]. Hence, the material could be suitable for applications where more flexible material is required such as in flexible solar cell [14].

3.2 ELECTRONIC PROPERTIES

The electronic band structure of $Cs_2InSbCl_6$ and $Cs_2In_{-x}SbCl_6$was calculated as shown in Figure 1(a) and 1(b) respectively using the projected augmented wave (PAW) within DFT-GGA functionals. The high symmetry directions (X - Γ - W - Γ - L) of the Brillouin zone were used throughout the calculation. It is observed that the parent material demonstrates semiconducting behavior. It clearly reveals the

presence of both the valence band maximum (VBM) and the conduction band minimum (CBM) at same symmetry (Γ-point) which confirm a direct band gap nature of the material (Figure 2(a)). The band gap was calculated to be 0.99 eV which is in excellent agreement with the value of 0.98 eV obtained by [1] and more recently 1.02 eV obtained by [15]. It is observed that the creation of indium vacancy shrinks the band gap with an overlap of electrons in the Γ – W – Γ symmetry (Figure 2(b)) hence exhibiting metallic behavior. Consequently, the density of state (DOS) provides an idea on how the energy gap of the material exists. It reveals details about the number of available states in the system, the amount of the allowed electron (hole) states per volume at given energy. Thus, it is a key essential tool for determining the energy distributions and carrier concentrations within semiconductor [14].

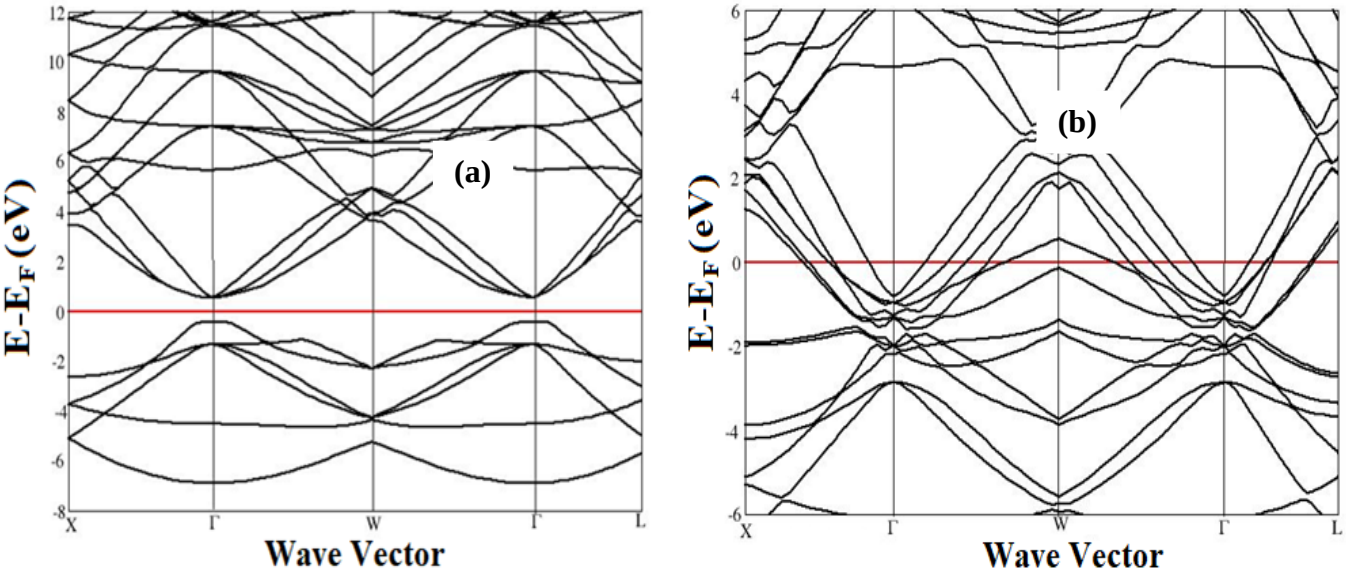

Figure 2: (a) Band structure of $Cs_2InSbCl_6$ (b) Band structure of $Cs_2In_{-x}SbCl_6$

The plotted DOS (Figure 3(a)) also reveals the semi conducting behavior of $Cs_2InSbCl_6$ and (Figure 3(b)) reveals metallic behavior of the indium vacancy created compound ($Cs_2In_{-x}SbCl_6$) respectively. It clearly shows the existence of energy range below the Fermi energy level (0 eV). It shows that the higher peaks are situated at the valence band for $Cs_2InSbCl_6$ and at conduction band for $Cs_2In_{-x}SbCl_6$. This indicates the presence of many electrons at the particular energy state.

The partial density of state (PDOS) plot (Figure 3(c)), it can be clearly observed that the vacancy causes a flatter band structure which lead to charge localization and, possibly cause the occurrence of self-trapped exciton [16]. The PDOS indicate that *s* and *p* orbitals of Cs are associated with the valence band maximum (VBM) and conduction band minimum (CBM) respectively. Also,VBM and CBM are contributed from both *s* and *p*-orbitals of the halide (Cl) and *p* and d-orbitals of transition metal (In). Thus, these contributions tuned the bandgap of the compounds to achieve the optimal region for a particular optoelectronic which could be done by mixing the halides or transition metals.

3.3 OPTICAL PROPERTIES

The study of optical properties involves the finding of material response to an applied electromagnetic field particularly to visible light [17].The knowledge is essential in determination of the efficiency of photovoltaic materials. Theoretically, an important function used in solid state physics to determine the linear response is the complex dielectric function [18]. The dielectric function $\varepsilon(\omega) = \varepsilon_1(\omega) + i\varepsilon_2(\omega)$ (where $\varepsilon_1(\omega)$ is the real part and $i\varepsilon_2(\omega)$ is the imaginary part) of the materials were calculated within the linear response TDDFT. The optical transition mechanism is illustrated by the imaginary part of the dielectric function. A greater value for dielectric constant of material indicates that the material has comparatively low charge carrier recombination rate and as such the entire performance

of the optoelectronics material will be improved [14]. The result obtained for $Cs_2InSbCl_6$ (Figure 4(a)) shows that the value of the imaginary part (ε_2) becomes zero at about 12.5 eV. This means that the material becomes transparent above 12.5 eV [17]. Generally, the value of ε_2 becomes nonzero once absorption starts. It can be seen that for ε_2 the main peaks are located 1.5 eV, 4 eV, and 6.5 eV (Figure 4(a)). An important remark to make from the real part (ε_1) plot is that ε_1 decreases to negative values. The negative values of (ε_1) indicates that at the particular energy level, there is mostly rejection of the incidence electromagnetic waves from the medium, as such the material exhibit metallic behavior [17]. As such it serves as protective means from radiations in the energy region. Comparing the result with the vacancy created compound ($Cs_2In_{-x}SbCl_6$) Figure 4(b) shows that the vacancy created material will absorb radiations up to about 9 eV which is lower than the initial compound (12.5 eV). This is in line with the difference in the electronic band nature obtained from the band structure (Figure 2(a) and (b)). Also, the high peaks of the imaginary part were located at 3 eV, 4 eV, and 4.5 eV respectively. This means that there will be higher absorption in a bit higher energy region when compared to the initial compound. The simulated result suggest that the material has a high transparency and hence less absorption in the high energy region (above 9 eV).

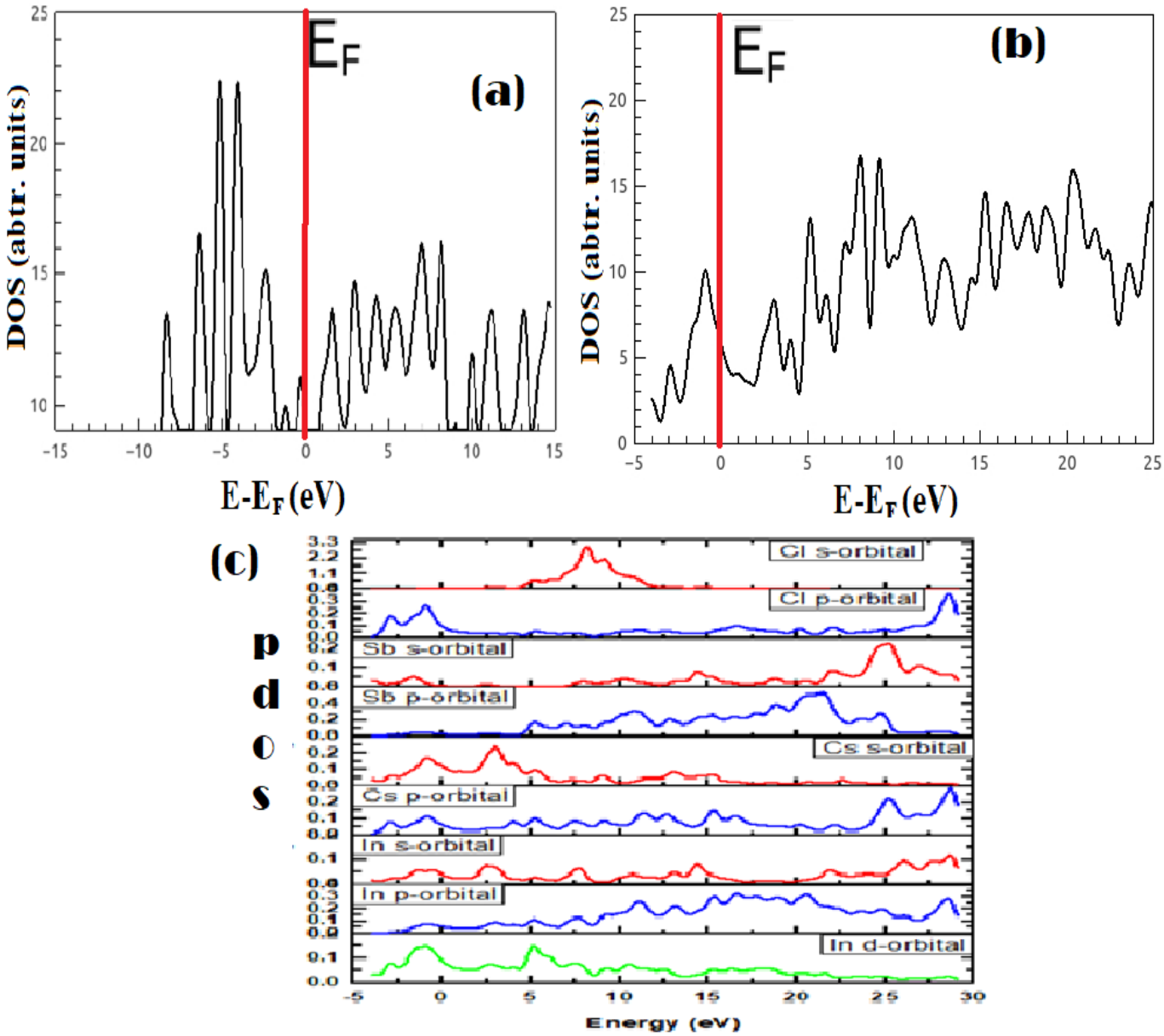

Figure 3: (a) Density of State for $Cs_2InSbCl_6$ (b) Density of State for $Cs_2In_{-x}SbCl_6$ (c) Partial Density of state for $Cs_2In_{-x}SbCl_6$

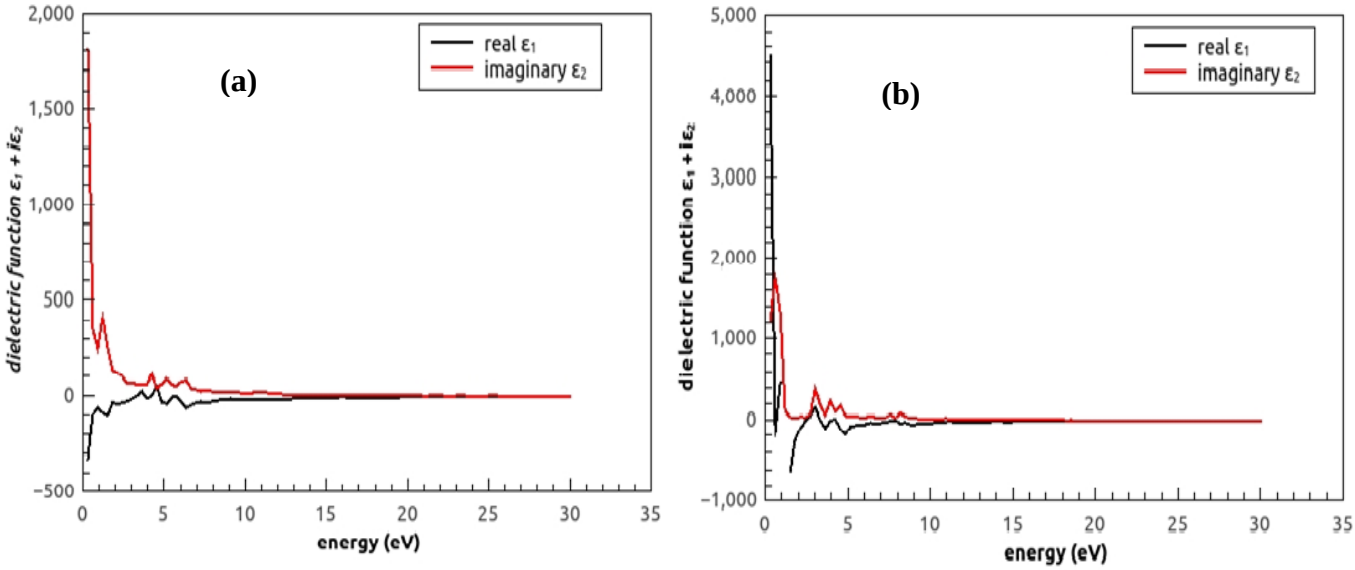

Figure 4: Dielectric Functions of (a) $Cs_2InSbCl_6$ (b) $Cs_2In_{-x}SbCl_6$

The absorption coefficient spectrum provides knowledge on the extent at which material absorbs photons. It indicates how far the light of a specific energy can penetrate into a material before being absorbed [12]. Figure 5(a) shows the absorption coefficient graph which provides information about optimum solar energy conversion efficiency. It reveals the absorption spectra for $Cs_2InSbCl_6$ and $Cs_2In_{-x}SbCl_6$. The absorption abruptly rises for energies higher than 0.5 eV which is in line with the band gap energy value. The absorption values are in the order of $10^4 cm^{-1}$ from the infrared to visible and down to the ultraviolet range (1.24 eV to 1.7 eV to above 3.3 eV). Several peaks were noticed to exist with $Cs_2InSbCl_6$ having its highest peak located just within the infrared energy region while the vacancy created compound $Cs_2In_{-x}SbCl_6$ was noticed to having its highest peak located just below the infrared region. This is in accordance with the metallic behavior exhibited by the material (Figure 2(b)). This affirms the result obtained by the DFT calculation of the electronic band structure (figure 2(a) & (b)) which reveals that the compound $Cs_2InSbCl_6$ is a semiconductor and that $Cs_2In_{-x}SbCl_6$ has metallic behavior. This is evidently the reason for the difference in the energy range of the highest peaks. An important remark to make is that the reference material $Cs_2InSbCl_6$ has higher peak in the high energy region, this makes it a good absorber material and as such it is considered as a better candidate for photovoltaic applications.

The electron energy loss function EELS is a vital optical parameter used in explaining the energy loss of a fast electron traversing a material which is large at plasma frequency [17]. Figure 5 (b) represent the corresponding EELS in function of photon energy of the materials. The prominent peaks were found to be at 28.02 eV for $Cs_2InSbCl_6$ and 11.5 eV for $Cs_2In_{-x}SbCl_6$. The sharp maxima peak for EELS indicates the existence of plasma resonance which appears at a specific incident light frequency which corresponds to the trailing edges in the reflection spectra often called plasma frequency (ω_p). The imaginary part of the dielectric function is zero at this point of energy which indicates rapid reduction in reflectance [18].

Reflectivity is an important optical parameter used to describe the ratio of reflected photon energy from material surface to the photon energy incident on the surface. Figure 5 (c) shows the reflectivity of the materials ($Cs_2InSbCl_6$ and $Cs_2In_{-x}SbCl_6$) as function of photon energy. The first edges were found to be at 90%, and 95% for $Cs_2InSbCl_6$, and $Cs_2In_{-x}SbCl_6$ respectively. These edges were noticed to be within the low energy level. The reflectivity begins to decrease as the energy increases from infrared region. It then increases to other peaks of 85, and 70 percent for $Cs_2In_{-x}SbCl_6$ and $Cs_2InSbCl_6$ respectively. These peaks were found to be located from visible to ultraviolet energy range. Another high peak of about 60% for $Cs_2In_{-x}SbCl_6$ was noticed in the far ultraviolet energy region (7.75 eV). The decrease in the reflectivity in the high energy region means that the material is transmitting in the ultraviolet wavelength as a result of lower reflectance within the energy

range. An important remark to make is that, the compound ($Cs_2In_{-x}SbCl_6$) with high reflectivity in the high energy region can be used as a good coating material to avoid solar heating [17].

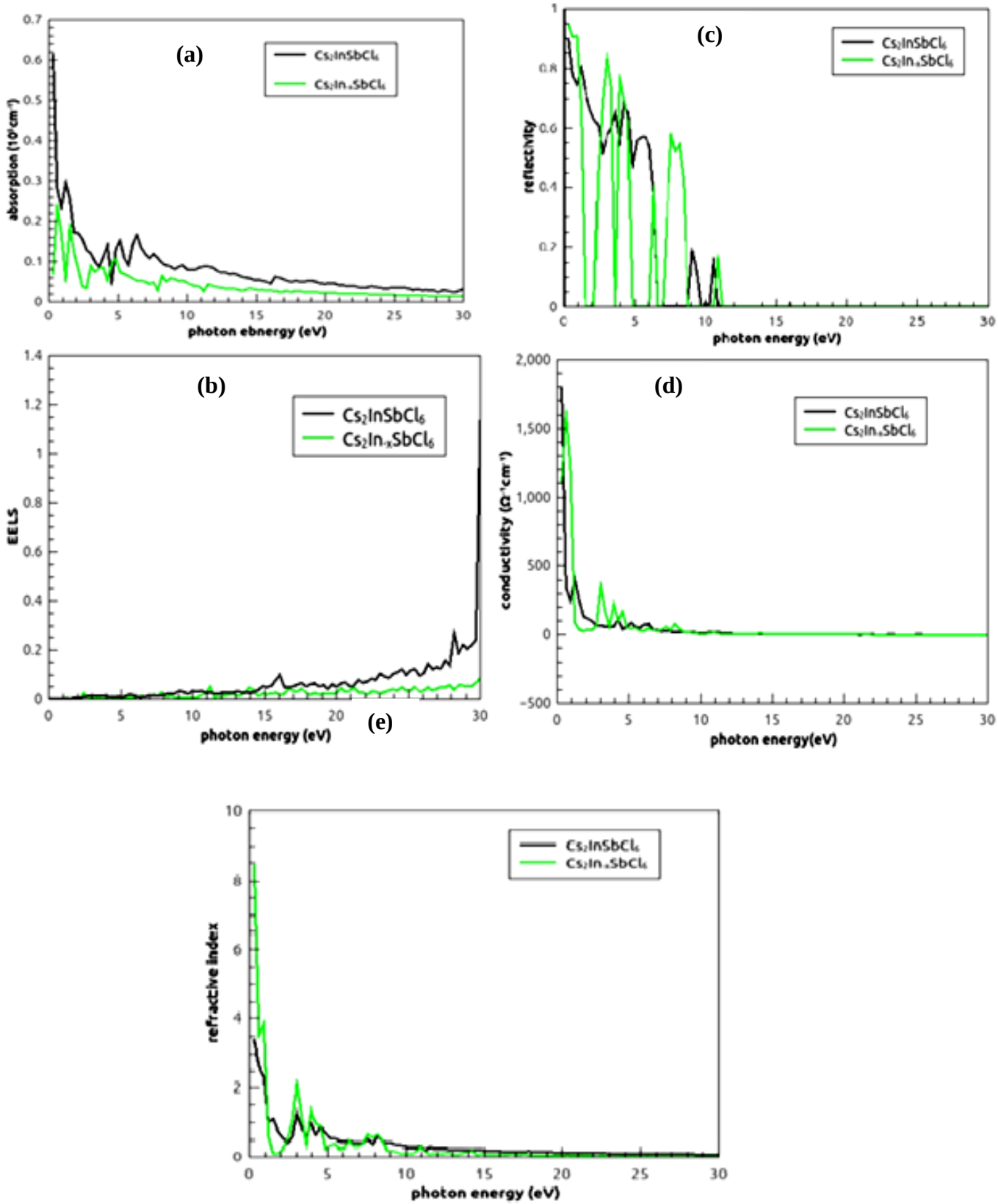

Figure 5: (a) Absorption Coefficient, (b) Electron Energy Loss Spectra, (c) Reflectivity, (d) Conductivity, (e) Refractive Index

Conductivity is an important optical property that provides information on the electrical conductivity of material. The measure of ease at which heat or electric charge pass through a material is termed conductivity. Figure 5 (d) shows the conductivity of the materials. It is observed that the material $Cs_2InSbCl_6$ has its own highest optical conductivity value of 1800 $\Omega^{-1}cm^{-1}$. The conductivity lowers to 1650 $\Omega^{-1}cm^{-1}$ at low energy level for $Cs_2In_{-x}SbCl_6$. The metallic behavior shown by the defect material in the band structure (Figure 2(b)) gives rise to several peaks in a bit higher energy region. Generally, material with higher photoconductivity is considered good candidate for photovoltaic applications.

The refractive index of a material is a dimensionless quantity which describes how much light travels or refracted after entering a material [18]. Figure 5(e) shows the refractive index n (ω) as a function of photon energy for $Cs_2In_{-x}SbCl_6$ and $Cs_2InSbCl_6$. The static refractive index n (0) was found to be 3.4 and 8.5 for $Cs_2InSbCl_6$ and $Cs_2In_{-x}SbCl_6$, respectively. From the graph, the materials possess a high refractive index at infrared region around (1.24 eV-1.7 eV) to visible region (1.7 eV-3.3 eV) and drastically decrease at higher energy from the visible to ultraviolet region (above 3.3eV). Furthermore, after 1.5 eV and 2.5 eV, the velocity of light is greater than the light celerity because n (ω) is less than one for $Cs_2In_{-x}SbCl_6$ and $Cs_2InSbCl_6$ respectively. The high value of n (0) attain by $Cs_2In_{-x}SbCl_6$ (8.5) means that the material becomes denser after defect and that the light entering the material will bend more towards the normal line. While on the other hand $Cs_2InSbCl_6$ having lower value of n (0) (3.4) will be less dense as such, the light rays will bend more away from the normal line.

4.0 CONCLUSION

A vacancy point defect was created in the indium site of the reference compound. The result of the structural investigation shows that the defect compound ($Cs_2In_{-x}SbCl_6$) is likely to be more stable compared to the reference compound ($Cs_2InSbCl_6$). It is also more compressible and hence could be suitable for where more flexibility and stability is required. The electronic band structure (Figure 2) shows that the vacancy point defect created shrinks the band gap (from what value to what value) with an overlap of electrons along the Γ - W – Γ symmetry thereby making the defect compound to behave in metallic nature. The optical properties calculation shows that the defect material ($Cs_2In_{-x}SbCl_6$) has lower absorption coefficient, high refractive index, high reflectivity and lower electrical conductivity when compared to the initial material. The outcome of the investigation placed the defect material not to be a better solar cell absorber material than the reference material, though could be more suitable where flexibility and stability is needed than the non defect material.

REFERENCE

[1] Xiao, Z., Du, K. Z., Meng, W., Wang, J., Mitzi, D. B., and Yan, Y. "Intrinsic instability of Cs2In (I) M (III) X6 (M= Bi, Sb; X= halogen) double perovskites: a combined density functional theory and experimental study" Journal of the American Chemical Society, vol. 139, pp. 6054-6057, 2017.

[2] Yu, H., Lu, H., Xie, F., Zhou, S., and Zhao, N. "Native defect-induced hysteresis behavior in organolead iodide perovskite solar cells" Advanced Functional Materials, vol. 26, pp. 1411-1419, 2015.

[3] Yu, H., Wang, F., Xie, F., Li, W., Chen, J., and Zhao, N. "The role of chlorine in the formation process of 'CH3NH3PbI3-xClx' perovskite" Advanced Functional Materials, vol. 24, pp. 7102-7108, 2014.

[4] Shi, J., and Yun, S. "First principle DFT calculations for perovskite solar cell" Wiley-VCH & Co. vol. 19, pp. 487-509, 2018.

[5] Prasadh D. P., and Sarkar, B. K. "Ab Initio Study of Electronic, Structural, Thermal and Mechanical Characterization of Cadmium Chalcogenides.Mechanics" Materials Science & Engineering Journal, vol 9, 2017.

[6] Kohn, W., and Sham, L. J. "Self-consistent equations including exchange and correlation effects" Physical review, vol. 140, 1965.

[7] Runge, E., and Gross, E. K. "Density-functional theory for time-dependent systems" *Physical Review Letters*, vol. *52*, pp. 997, 1984.

[8] Giannozzi, P., Baroni, S., Bonini, N., Calandra, M., Car, R., Cavazzoni, C., and Dabo, I. "QUANTUM ESPRESSO: a modular and open-source software project for quantum simulations of materials" Journal of Physics: Condensed Matter, vol. 21, pp. 395502, 2009.

[9] Perdew, J. P., Burke, K., and Ernzerhof, M. "Generalized gradient approximation made simple" *Physical review letters*, vol. *77*, pp. 3865, 1996.

[10] Fletcher, R. "Practical methods of optimization" John Wiley & Sons, 2013.

[11] King R.C. "Introduction to microelectronics theory" Georgia institute of technology, 2005.

[12] Houari, M., Bouadjemi, B., Abbad, A., Benstaali, W., Haid, S., Lantri, T., ... and Aziz, Z. "Structural, electronic and optical properties of cubic fluoroelpasolite Cs2NaYF6 by density functional theory" *Chinese Journal of Physics*, vol. *56*, pp. 1756-1763, 2018.

[13] Gao, L. K., Tang, Y. L., and Diao, X. F. "First-Principles Study on the Photoelectric Properties of CsGeI3 under Hydrostatic Pressure" *Applied Sciences*, vol. *10*, pp. 5055, 2020.

[14] Islam, J., and Hossain, A. A. "Narrowing band gap and enhanced visible-light absorption of metal-doped non-toxic CsSnCl3 metal halides for potential optoelectronic applications" RSC Advances, vol. 10, pp. 7817-7827, 2020.

[15] Li, Y. "First-Principles Study of Hybrid Halide Perovskites and Beyond for Optoelectronic Applications" (Doctoral dissertation, UC San Diego), 2020.

[16] Kaewmeechai, C., Laosiritaworn, Y., and Jaroenjittichai, A. P. "DFT calculation on electronic properties of vacancy-ordered double perovskites Cs2 (Ti, Zr, Hf) X6 and their alloys: Potential as light absorbers in solar cells" *Results in Physics*, vol. *30*, pp. 104875, 2021.

[17] Rahman, M. A., Rahaman, M. Z., and Rahman, M. A. "The structural, elastic, electronic and optical properties of MgCu under pressure: A first-principles study" International Journal of Modern Physics B, vol. 30, pp. 1650199, 2016.

[18] Lawal, A., Shaari, A., Ahmed, R., and Jarkoni, N. "First-principles investigations of electron-hole inclusion effects on optoelectronic properties of Bi2Te3, a topological insulator for broadband photodetector" Physica B: Condensed Matter, vol. 520, pp. 69-75, 2017. https://www.youtube.com/watch?v=DKHffCHSoAk